Inorg. Chem. **2006**, *45*, 5785–5792

Modulated Preparation and Structural Diversification of Zn^{II} and Cd^{II} Metal–Organic Frameworks with a Versatile Building Block 5-(4-Pyridyl)-1,3,4-oxadiazole-2-thiol

Miao Du,*,† Zhi-Hui Zhang,† Xiao-Jun Zhao,† and Qiang Xu‡

College of Chemistry and Life Science, Tianjin Normal University, Tianjin 300074, P. R. China, and National Institute of Advanced Industrial Science and Technology (AIST), Ikeda, Osaka 563-8577, Japan

Received January 22, 2006

Four novel Zn^{II} and Cd^{II} metal–organic coordination polymers with a versatile building block 5-(4-pyridyl)-1,3,4-oxadiazole-2-thiol (Hpyt) have been prepared under different conditions. $[Zn_3(pyt)_4(OH)_2]_n$ (**1**) and $[Cd(pyt)(HCOO)]_n$ (**3**) were obtained through a solvothermal method, whereas $\{[Zn(pyt)_2(H_2O)_2]\cdot(DMF)_2\}_n$ (**2**) and $\{[Cd(pyt)_2]\cdot CHCl_3\}_n$ (**4**) were isolated under general conditions. X-ray single-crystal diffraction indicates that the anionic ligand pyt adopts a thioamide isomer in **1**, **2**, and **4**, but a thiolate form in **3**. Four types of binding modes involving monodentate (η-N_{oxa}), bidentate (μ-N_{py},N_{oxa}, or μ-N_{py},S,S) and tridentate (μ-N_{py},N_{oxa},S) are observed. The discrepancy of the synthetic routes and metal-coordination preferences facilitates the production of the final crystalline materials with distinct network structures, including a 1D zigzag array of **1** with dangling arms, a common 2D (4,4) coordination layer of **2**, a decorated 3D α-Po network of **3**, and an unprecedented (3,6)-connected 3D framework of **4** with a $(4^2.6)_2(4^2.6^2.8^7.10^2)$ topology. Notably, the hydrolysis of DMF solvates leads to the formation of formate ions, being a component in the structure of **3**. Complexes **2** and **4** show 1D channels in which the solvates are accommodated, and even after the exclusion of these guests, the porous host frameworks are still retained. Thermal stability and gas adsorption properties have also been studied.

Introduction

The deliberate design of metal−organic crystalline materials has attracted considerable attention for their interesting supramolecular architectures and tailor-made applications in porosity, magnetism, optoelectronics, and catalysis.[1,2] As is widely known, the structural and functional information of such target materials significantly rests with the metal and ligand precursors.[1,2] In this aspect, a variety of organic building blocks containing pyridyl and/or carboxylate functional groups have been intensely investigated,[1−3] and the design of new types of organic ligands for constructing unusual coordination polymers is obviously not trivial at this stage. Heterocyclic thiones represent an important type of compounds in the field of coordination chemistry, a majority of which involve α-N-donor[4] or β-N-donor[5] thione/thiolate species because of their potential multifunctional donors of either exocyclic sulfur or heterocyclic nitrogen. Very recently, increasing numbers of investigations have been focused on the self-assembly of such multidentate N,S-donor ligands with metal ions in different ways. This leads to the formation of either discrete polynuclear complexes or infinite coordination polymers,[4−6] which display such useful proper-

* To whom correspondence should be addressed. Fax: 86-22-23540315. Tel: 86-22-23538221. E-mail: dumiao@public.tpt.tj.cn.
† Tianjin Normal University.
‡ National Institute of Advanced Industrial Science and Technology.

(1) (a) Hoskins, B. F.; Robson, R. *J. Am. Chem. Soc.* **1990**, *112*, 1546−1554. (b) Batten, S. R.; Robson, R. *Angew. Chem., Int. Ed.* **1998**, *37*, 1460−1494. (c) Janiak, C. *Dalton Trans.* **2003**, 2781−2804. (d) Yaghi, O. M.; O'Keeffe, M.; Ockwig, N. W.; Chae, H. K.; Eddaoudi, M.; Kim, J. *Nature* **2003**, *423*, 705−714. (e) Brammer, L. *Chem. Soc. Rev.* **2004**, *33*, 476−489. (f) Ockwig, N. W.; Delgado-Friedrichs, O.; O'Keeffe, M.; Yaghi, O. M. *Acc. Chem. Res.* **2005**, *38*, 176−182.
(2) (a) Moulton, B.; Zaworotko, M. J. *Chem. Rev.* **2001**, *101*, 1629−1658. (b) Evans, O. R.; Lin, W. *Acc. Chem. Res.* **2002**, *35*, 511−522. (c) Carlucci, L.; Ciani, G.; Proserpio, D. M. *Coord. Chem. Rev.* **2003**, *246*, 247−289. (d) Batten, S. R.; Murray, K. S. *Coord. Chem. Rev.* **2003**, *246*, 103−130. (e) Kitagawa, S.; Kitaura, R.; Noro, S. *Angew. Chem., Int. Ed.* **2004**, *43*, 2334−2375. (f) Bradshaw, D.; Claridge, J. B.; Cussen, E. J.; Prior, T. J.; Rosseinsky, M. J. *Acc. Chem. Res.* **2005**, *38*, 273−282. (g) Lin, W. *J. Solid State Chem.* **2005**, *178*, 2846−2490.
(3) (a) Barnett, S. A.; Champness, N. R. *Coord. Chem. Rev.* **2003**, *246*, 145−168. (b) Rao, C. N. R.; Natarajan, S.; Vaidhyanathan, R. *Angew. Chem., Int. Ed.* **2004**, *43*, 1466−1496. (c) Ye, B. H.; Tong, M. L.; Chen, X. M. *Coord. Chem. Rev.* **2005**, *249*, 545−565.
(4) (a) Garcia-Vazquez, J. A.; Romero, J.; Sousa, A. *Coord. Chem. Rev.* **1999**, *193-5*, 691−745. (b) Akrivos, P. D. *Coord. Chem. Rev.* **2001**, *213*, 181−210.
(5) Fleischer, H. *Coord. Chem. Rev.* **2005**, *249*, 799−827.

10.1021/ic060129v CCC: $33.50
Published on Web 06/21/2006

Scheme 1

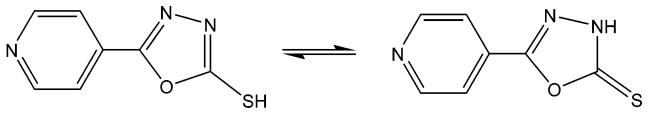

ties as semiconductivity, photoluminescence, and biomimicry. Meanwhile, pyridyl oxadiazole compounds have also been systematically explored for their potential biological activities[7] and luminescence properties,[8] as well as the promising bridging ligands for coordination chemistry.[9]

Considering all stated above, an interesting building block 5-(4-pyridyl)-1,3,4-oxadiazole-2-thiol (Hpyt), in which the central ring system 1,3,4-oxadiazole is substituted with pyridyl and thiol functional pendants, attracts our attention for achieving new polymeric coordination networks with diverse metal ions. X-ray diffraction study reveals that the free Hpyt molecule exists in a thione form in the solid state,[10] although two potential isomers (thiol vs thione) are possible (see Scheme 1). Presumably, a variety of coordination modes may be anticipated for it because of its changeable conformations and multiple interaction sites. Curiously, the coordination chemistry of Hpyt has been unexplored so far, probably because of its poor solubility in water and common organic solvents. To facilitate the generation and crystallization of metal complexes with Hpyt, we introduce in our present research the solvothermal synthetic method that has been testified to be powerful in preparing the low-soluble inorganic−organic hybrid materials.[11] A 1D zigzag chain $[Zn_3(pyt)_4(OH)_2]_n$ (**1**) with trinuclear Zn^{II} subunits and a 3D pillar-layered framework $[Cd(pyt)(HCOO)]_n$ (**3**) with a decorated α-Po net topology have been obtained in a mixed $H_2O/DMF/CHCl_3$ medium under solvothermal conditions. Notably, the anionic formate ligands in **3** arise from the hydrolysis of DMF. On the other hand, it is fortunate that a 2D gridlike layered complex $\{[Zn(pyt)_2(H_2O)_2]\cdot(DMF)_2\}_n$ (**2**) and a 3D coordination polymer $\{[Cd(pyt)_2]\cdot CHCl_3\}_n$ (**4**) with a new (3,6)-connected $(4^2.6)_2(4^4.6^2.8^7.10^2)$ net topology have also been isolated from the same starting reagents under spontaneous self-assembly. To our pleasant surprise, the variation of the experimental conditions and metal ions lead to the formation of distinct products with various network structures from 1D to 3D. The versatility of the pyt anion in **1**−**4**, including the changeable ligand configurations and diverse binding fashions, is also discussed in detail. These results reveal that such a type of multidentate module is a useful building block and may open a new avenue for coordination polymer chemistry.

Experimental Section

General Materials and Methods. All starting reagents were obtained commercially and used as received. FT-IR spectra (KBr pellets) were taken on an AVATAR-370 (Nicolet) spectrometer. Elemental analyses were performed on a CE-440 (Leemanlabs) analyzer. Thermogravimetric analysis (TGA) experiments were carried out on a Dupont thermal analyzer from 20 to 800 °C under N_2 at a heating rate of 10 °C/min. X-ray powder diffraction (XRPD) patterns were recorded on a Rigaku D/max-2500 diffractometer with Cu Kα radiation (λ = 1.5406 Å). Nitrogen adsorption isotherms were measured using the automatic volumetric adsorption equipment (ASAP2010, Shimadzu).

Syntheses of Complexes 1−4. $[Zn_3(pyt)_4(OH)_2]_n$ (1). A mixture of $Zn(OAc)_2\cdot 2H_2O$ (22 mg, 0.1 mmol) and Hpyt (18 mg, 0.1 mmol) in $H_2O/DMF/CHCl_3$ (10 mL) was sealed in a Teflon-lined stainless steel vessel (20 mL) and heated to 100 °C for 1 day. It was then gradually cooled to room temperature at a rate of 1 °C/h, giving pale-yellow block crystals in a 67% yield (16 mg, on the basis of Hpyt). Anal. Calcd for $C_{28}H_{18}Zn_3N_{12}O_6S_4$: C, 35.67; H, 1.92; N, 17.83. Found: C, 35.89; H, 1.79; N, 17.81. IR (cm^{-1}): 3434b, 1624s, 1542w, 1493w, 1416vs, 1378vs, 1220m, 1193s, 1088m, 1060m, 1023w, 973w, 874m, 832m, 724w, 701m, 541m.

$\{[Zn(pyt)_2(H_2O)_2]\cdot(DMF)_2\}_n$ (2). A water solution (5 mL) of $Zn(OAc)_2\cdot 2H_2O$ (22 mg, 0.1 mmol) was carefully layered onto a $CHCl_3$/DMF medium (6 mL), below which was placed Hpyt solid (18 mg, 0.1 mmol) at the bottom of a straight glass tube. Upon slow evaporation of the solvents, pale yellow lamellar crystals were produced after 3 weeks in a yield of 51% (15 mg, on the basis of Hpyt). Anal. Calcd for $C_{20}H_{26}ZnN_8O_6S_2$: C, 39.77; H, 4.34; N, 18.55. Found: C, 39.86; H, 4.20; N, 18.44. IR (cm^{-1}): 3412b, 3202s, 1670s, 1617s, 1544w, 1493w, 1427s, 1373vs, 1219w, 1169s, 1091m, 1060w, 1012m, 953w, 841m, 719m, 701m, 663w, 545w, 524w, 489w.

$[Cd(pyt)(HCOO)]_n$ (3). The same method as that for **1** was used except the metal salt was replaced by $Cd(OAc)_2\cdot 2H_2O$ (27 mg, 0.1 mmol), affording colorless sheet single crystals in a 57% yield (19 mg, on the basis of Hpyt). Anal. Calcd for $C_8H_5CdN_3O_3S$: C, 28.63; H, 1.50; N, 12.52. Found: C, 28.47; H, 1.74; N, 12.61. IR (cm^{-1}): 1612s, 1564vs, 1480w, 1423vs, 1392s, 1342s, 1213m, 1146m, 1077w, 1053w, 996w, 842m, 786m, 705m, 524m.

$\{[Cd(pyt)_2]\cdot CHCl_3\}_n$ (4). The same method as that for **2** was used except that the metal salt was replaced by $Cd(OAc)_2\cdot 2H_2O$ (27 mg, 0.1 mmol), giving colorless block single crystals after 2 weeks in a yield of 78% (23 mg, on the basis of Hpyt). Anal. Calcd for $C_{15}H_9CdN_6O_2S_2Cl_3$: C, 30.63; H, 1.54; N, 14.29. Found: C, 30.78; H, 1.50; N, 14.47. IR (cm^{-1}): 1614m, 1544s, 1418vs, 1217w, 1167m, 1083w, 1058w, 1005w, 832w, 710m, 689m, 616w, 540w.

X-ray Crystallography. Single-crystal X-ray diffraction measurements for **1**−**4** were performed on a Bruker Apex II CCD diffractometer equipped with graphite-monochromated Mo Kα radiation (λ = 0.71073 Å). There was no evidence of crystal decay during data collection. Semiempirical absorption corrections were applied (SADABS) and the program SAINT was used for integration of the diffraction profiles.[12] The structures were solved by direct methods using SHELXS and refined with SHELXL.[13] The non-H atoms were modeled with anisotropic parameters and refined by full-matrix least-squares methods on F^2. Carbon-bound H atoms were placed geometrically and refined as the riding atoms. In the structures of **1** and **2**, the starting positions for hydroxyl or water

(6) (a) Zhao, Y.; Hong, M.; Liang, Y.; Cao, R.; Li, W.; Weng, J.; Lu, S. *Chem. Commun*. **2001**, 1020−1021. (b) Lobana, T. S.; Sharma, R.; Bermejo, E.; Castineiras, A. *Inorg. Chem.* **2003**, *42*, 7728−7730. (c) Lobana, T. S.; Sharma, R.; Sharma, R.; Mehra, S.; Castineiras, A.; Turner, P. *Inorg. Chem.* **2005**, *44*, 1914−1921. (d) Li, D.; Shi, W.-J.; Hou, L. *Inorg. Chem.* **2005**, *44*, 3907−3913.

(7) Nofal, Z. M.; Fahmy, H. H.; Mohamed, H. S. *Arch. Pharm. Res.* **2002**, *25*, 250−257.

(8) Abou-Elenien, G. M.; Ismail, N. A.; El-Maghraby, A. A.; Al-abdallah, G. M. *Electroanalysis* **2001**, *13*, 1022−1029.

(9) Nuriev, V. N.; Zyk, N. V.; Vatsadze, S. Z. *ARKIVOC* **2005**, 208−224.

(10) Du, M.; Zhao, X.-J.; Guo, J.-H. *Acta Crystallogr., Sect. E* **2004**, *60*, o327−o328.

(11) Feng, S.; Xu, R. *Acc. Chem. Res.* **2001**, *34*, 239−247.

(12) *SAINT Software Reference Manual*; Bruker AXS: Madison, WI, 1998.

(13) Sheldrick, G. M. *SHELXTL NT, Program for Solution and Refinement of Crystal Structures*, version 5.1; University of Göttingen: Göttingen, Germany, 1997.

Table 1. Crystallographic Data and Structure Refinement Summary for Complexes **1**−**4**

	1	**2**	**3**	**4**
chemical formula	$C_{28}H_{18}Zn_3N_{12}O_6S_4$	$C_{20}H_{26}ZnN_8O_6S_2$	$C_8H_5CdN_3O_3S$	$C_{15}H_9CdN_6O_2S_2Cl_3$
fw	942.89	603.98	335.61	588.15
cryst size (mm^3)	0.48 × 0.36 × 0.28	0.54 × 0.48 × 0.20	0.46 × 0.43 × 0.16	0.32 × 0.26 × 0.14
cryst syst	monoclinic	monoclinic	monoclinic	monoclinic
space group	*C*2/*c*	$P2_1/n$	$P2_1/c$	$P2_1/c$
a (Å)	23.727(2)	8.815(4)	11.865(8)	11.6012(8)
b (Å)	9.2329(7)	12.671(5)	12.152(8)	16.858(1)
c (Å)	17.116(1)	11.906(5)	6.713(4)	10.9825(7)
β (deg)	112.242(1)	100.050(5)	102.896(8)	94.758(1)
V ($Å^3$)	3470.6(5)	1309.4(9)	944(1)	2140.5(2)
Z	4	2	4	4
ρ_{calcd} (g/cm^3)	1.805	1.532	2.363	1.825
μ (mm^{-1})	2.359	1.149	2.528	1.614
F(000)	1888	624	648	1152
no. of total/independent reflns	9108/3048	6870/2303	4974/1656	11 449/3766
no. of params	240	171	145	263
R_{int}	0.0191	0.0195	0.0194	0.0161
R^a, $R_w{}^b$	0.0210, 0.0522	0.0249, 0.0649	0.0172, 0.0456	0.0266, 0.0674
GOF[c]	1.010	1.071	1.063	1.042
residuals (e $Å^{-3}$)	0.232, −0.210	0.534, −0.240	0.339, −0.394	0.825, −0.799

[a] $R = \sum||F_o| - |F_c||/\sum|F_o|$. [b] $R_w = [\sum[w(F_o^2 - F_c^2)^2]/\sum w(F_o^2)^2]^{1/2}$. [c] $GOF = \{\sum[w(F_o^2 - F_c^2)^2]/(n - p)\}^{1/2}$.

H were located in difference Fourier syntheses and then fixed geometrically and included in the refinement. Further details for crystallographic data and refinement conditions are listed in Table 1.

Results and Discussion

Preparation and Characterization. The ligand Hpyt is insoluble in water and organic solvents such as acetonitrile, methanol, chloroform, and acetone but slightly soluble in DMF or THF. The direct-solution assembly of Hpyt with Zn^{II} or Cd^{II} acetate generates yellow or white microcrystalline precipitate. To obtain qualified crystals for X-ray determination, two synthetic strategies were undertaken. One is hydro/solvothermal technology, which has been widely applied in metal−organic frameworks preparation. Notably, such a complicated process is also attended by the unprecedented in situ organic reactions including ligand oxidative coupling, hydrolysis, and substitution.[14] In this work, **1** and **3** were produced via solvothermal synthesis and the hydrolysis of DMF was observed in the formation of **3**. From a chemical viewpoint, DMF hydrolysis is far from straightforward; however, this has been detected in a few examples for anionic coordination networks of aromatic carboxylates incorporating with the $NH_2Me_2^+$ template.[15] Significantly, the hydrolysis product formate ions act as a participant in the coordination framework of **3**, which, to the best of our knowledge, is unknown so far. Well-shaped single crystals of **2** or **4** were achieved by the diffusion method in mixed solvents. Unusually, the solid of Hpyt was directly placed at the bottom of the tube covered by $CHCl_3$/DMF instead of the aforementioned dissolution so as to facilitate the slow growth of larger single crystals for X-ray diffraction.

It is interesting that different crystalline products (**1** and **2** for Zn^{II}; **3** and **4** for Cd^{II}) were generated via two synthetic routes with the same reactants. The compositions of all new materials were validated by elemental analyses and IR spectra. The phase purities of the bulk samples were identified by XRPD (see the Supporting Information, Figure S1). It should be noted that complexes **1**−**3** are air-stable and can retain their structural integrity for a considerable length of time, whereas solvates loss occurs for **4** even at room temperature after a period of ca. 1 week, resulting in an opaque solid. Therefore, all characterization data of **4** were recorded using a fresh sample. In the IR spectra of **1** and **2**, a broad band centered at ca. 3400 cm^{-1} indicates the O−H characteristic stretching vibrations of hydroxyl or water. The absorption bands resulting from the skeletal vibrations of the aromatic rings of pyt for all the cases appear in 1400−1600 cm^{-1} area. The IR spectrum of **2** shows a strong absorption of carbonyl in 1670 cm^{-1}, indicating the presence of DMF. For **3**, the characteristic bands of formate appear at 1564 and 1423 cm^{-1}, respectively, being the antisymmetric and symmetric stretching vibrations of carboxylate.

Structural Analysis of Complexes 1−4. $[Zn_3(pyt)_4(OH)_2]_n$ (1). Complex **1** represents a 1D coordination array with trinuclear Zn^{II} subunits. The asymmetric unit is composed of one and a half Zn^{II} atoms, a hydroxyl, and a pair of anionic ligands (Figure 1a). Interestingly, both Zn^{II} ions have different coordination spheres (see Table 2 for detailed bond parameters). The half-occupied Zn1, locating at a 2-fold axis, is coordinated to two oxadiazole groups and two OH^- bridges. The resulting ZnN_2O_2 tetrahedral core shows a considerable distortion, which is reflected by a large angle of 117.74(9)° for O3A−Zn1−O3. Although Zn2 binds to four distinct functional groups, involving one pyridyl, one oxadiazole, a hydroxyl, and a sulfur donor, it also shows a distorted tetrahedral geometry (ZnN_2SO) with an O3−Zn2−N1 angle of 123.67(7)°. Thus, three Zn^{II} centers are linked by two pyt to result in a trinuclear unit, which is fixed by

(14) (a) Zhang, X.-M.; Tong, M.-L.; Chen, X.-M. *Angew. Chem., Int. Ed.* **2002**, *41*, 1029−1031. (b) Xiong, R.-G.; Xue, X.; Zhao, H.; You, X.-Z.; Abrahams, B. F.; Xue, Z.-L. *Angew. Chem., Int. Ed.* **2002**, *41*, 3800−3803. (c) Tong, M.-L.; Li, L.-J.; Mochizuki, K.; Chang, H.-C.; Chen, X.-M.; Li, Y.; Kitagawa, S. *Chem. Commun.* **2003**, 428−429. (d) Zhang, J.-P.; Zheng, S.-L.; Huang, X.-C.; Chen, X.-M. *Angew. Chem., Int. Ed.* **2004**, *43*, 206−209.

(15) (a) Chen, W.; Wang, J. Y.; Chen, C.; Yue, Q.; Yuan, H. M.; Chen, J. S.; Wang, S. N. *Inorg. Chem.* **2003**, *42*, 944−946. (b) Rosi, N. L.; Kim, J.; Eddaoudi, M.; Chen, B.; O'Keeffe, M.; Yaghi, O. M. *J. Am. Chem. Soc.* **2005**, *127*, 1504−1518. (c) Burrows, A. D.; Cassar, K.; Friend, R. M. W.; Mahon, M. F.; Rigby, S. P.; Warren, J. E. *CrystEngComm* **2005**, *7*, 548−550. (d) Xie, L.; Liu, S.; Gao, B.; Zhang, C.; Sun, C.; Li, D.; Su, Z. *Chem. Commun.* **2005**, 2402−2404.

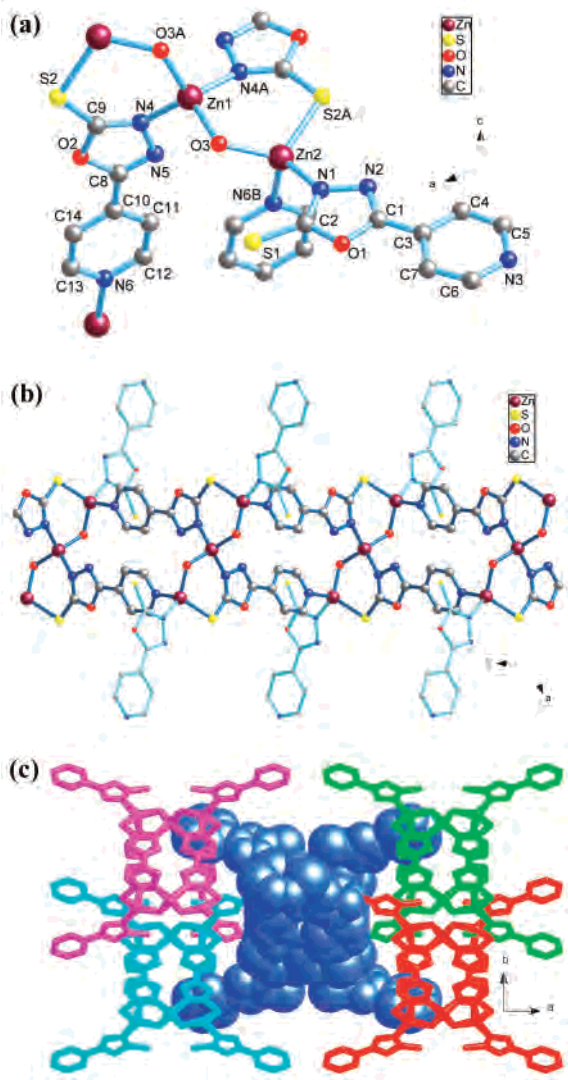

Figure 1. (a) Portion view of **1** with atom labeling of the asymmetric unit and metal-coordination sphere (hydrogen atoms are omitted for clarity). (b) 1D pyt-bridged double-chain array with trinuclear Zn^{II} units; the pyt terminals decorated as lateral arms are highlighted in cyan. (c) Sketch map showing the entangled packing of each 1D motif (in space-filling model) by four neighbors (in different colors).

hydroxyl. As a consequence, a couple of six-membered Zn−O−Zn−S−C−N rings are given with a Zn1···Zn2 separation of 3.2963(3) Å. Such an orbicular pattern is unknown in metal coordination, as suggested by a Cambridge Structural Database (CSD) search (version 5.27, Nov 2005).[16] These subunits are extended into a 1D double chain via further Zn−N_{py} coordination, which is decorated by the monodentate pyt ligands as the dangling arms (Figure 1b). In fact, this 1D motif is zigzag, with the terminal pyt locating at each turning point (see the Supporting Information, Figure S2). As for the ligands, two binding modes are observed though both pyt anions behave as the thioamide isomer with compressed C−S lengths and two unequal C−N bonds of oxadiazole (see Table 2). The pyridyl ring makes a dihedral angle of 1.7(1)° with oxadiazole for the unidentate pyt and the value

(16) Bruno, I. J.; Cole, J. C.; Edgington, P. R.; Kessler, M.; Macrae, C. F.; McCabe, P.; Pearson, J.; Taylor, R. *Acta Crystallogr., Sect. B* **2002**, *58*, 389−397.

Table 2. Selective Bond Lengths (Å) and Angles (deg) for Complexes **1** and **2**

		1[a]	
Zn1−O3	1.901(1)	Zn1−N4	2.038(2)
Zn2−N6B	2.060(2)	Zn2−S2A	2.3196(6)
Zn2−N1	1.978(2)	Zn2−O3	1.905(2)
C2−S1	1.658(2)	C9−S2	1.698(2)
C2−N1	1.307(3)	N2−C1	1.277(3)
C9−N4	1.308(2)	N5−C8	1.284(2)
O3A−Zn1−O3	117.74(9)	O3A−Zn1−N4A	111.28(6)
O3−Zn1−N4A	104.53(6)	O3A−Zn1−N4	104.53(6)
O3−Zn1−N4	111.28(6)	N4A−Zn1−N4	107.17(9)
O3−Zn2−N1	123.67(7)	O3−Zn2−N6B	100.12(7)
N1−Zn2−N6B	102.83(7)	O3−Zn2−S2A	113.26(5)
N1−Zn2−S2A	107.15(5)	N6B−Zn2−S2A	108.08(5)
N1−C2−S1	129.1(2)	N4−C9−S2	133.0(2)
		2[b]	
Zn1−N3	2.133(2)	Zn1−O3	2.136(1)
Zn1−N1B	2.218(2)	C7−S1	1.680(2)
C7−N3	1.318(2)	N2−C6	1.282(3)
N3−Zn1−O3	90.26(6)	N3A−Zn1−O3	89.74(6)
N3−Zn1−N1B	93.06(6)	N3A−Zn1−N1B	86.94(6)
O3A−Zn1−N1C	91.64(6)	O3−Zn1−N1C	88.36(6)
N3−C7−S1	130.9(1)		

[a] Symmetry codes: A = $-x+1$, y, $-z+1/2$; B = $-x+1$, $-y$, $-z$. [b] Symmetry codes: A = $-x$, $-y+2$, $-z+2$; B = $x-1/2$, $-y+3/2$, $z+1/2$; C = $-x+1/2$, $y+1/2$, $-z+3/2$.

is 13.2(1)° for the bridging one. Furthermore, each 1D motif is entangled with four neighboring ones (Figure 1c) without any significant interactions.

$\{[Zn(pyt)_2(H_2O)_2]\cdot(DMF)_2\}_n$ (2). The asymmetric unit of 2D layered complex **2** (see Figure 2a) contains one Zn^{II} atom that lies on an inversion center (at (0, 1, 1)), one pyt, and an aqua ligand, as well as the DMF solvates. The Zn^{II} ion has a nearly ideal octahedral geometry (see Table 2 for bond parameters), provided by four nitrogen donors from pyridyl and oxadiazole rings and two water ligands. Each pyt entity adopts the thioamide form (C7−S1 = 1.680(2) Å) and a bidentate bridging mode, within which the pyridyl ring is inclined to oxadiazole with a dihedral angle of 6.1(1)°. The Zn^{II} centers are extended by pyt ligands along two directions with a dimension of 10.21(1) $Å^2$, resulting in a 2D (4,4) layer with rhombic meshes. The angles of each $[Zn_4(pyt)_4]$ repeating unit are 76.745(2) and 103.255(2)°, and the diagonal Zn···Zn distances are 12.671(5) and 16.003(5) Å. Notably, these 2D layers stack in a parallel fashion, affording 1D channels along [100] (Figure 2b). Computation of the channel space using *PLATON*[17] suggests a value of 523.6 $Å^3$ (40.0% of the whole unit-cell volume), which is filled by the guest DMF molecules. Furthermore, this structure is also stabilized by host−guest O−H···O hydrogen bonds with the association of intralayer O−H···S interactions (see the Supporting Information, Table S1).

$[Cd(pyt)(HCOO)]_n$ (3). The structure of **3** presents a 3D pillar-layered framework. Each Cd^{II} atom coordinates to three pyt ligands and three formates, forming a $CdNO_3S_2$ disordered octahedral geometry (Figure 3a). Dissimilarly to that in **1** and **2**, pyt takes the thiolate style in this case and bridges the metal ions via pyridyl nitrogen and exocyclic sulfur donors. The C−S bond length is as long as 1.714(2) Å, and the two C−N distances are almost equivalent (Table 3), with a dihedral angle of 8.1(1)° between the pyridyl and oxadia-

(17) Spek, A. L. *J. Appl. Crystallogr.* **2003**, *36*, 7−13.

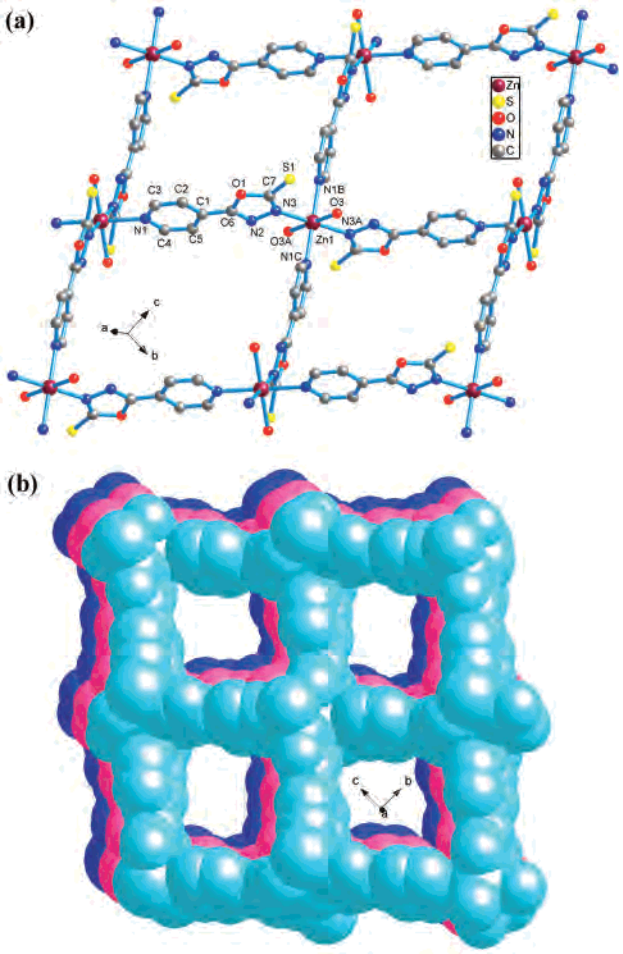

Figure 2. (a) Single (4,4) coordination layer in the structure of **2** with atom labeling of the asymmetric unit and metal-coordination sphere (hydrogen atoms and lattice DMF solvates are omitted for clarity). (b) Packing diagram of **2** showing 1D square channels along the [100] direction; three adjacent layers are indicated by different colors.

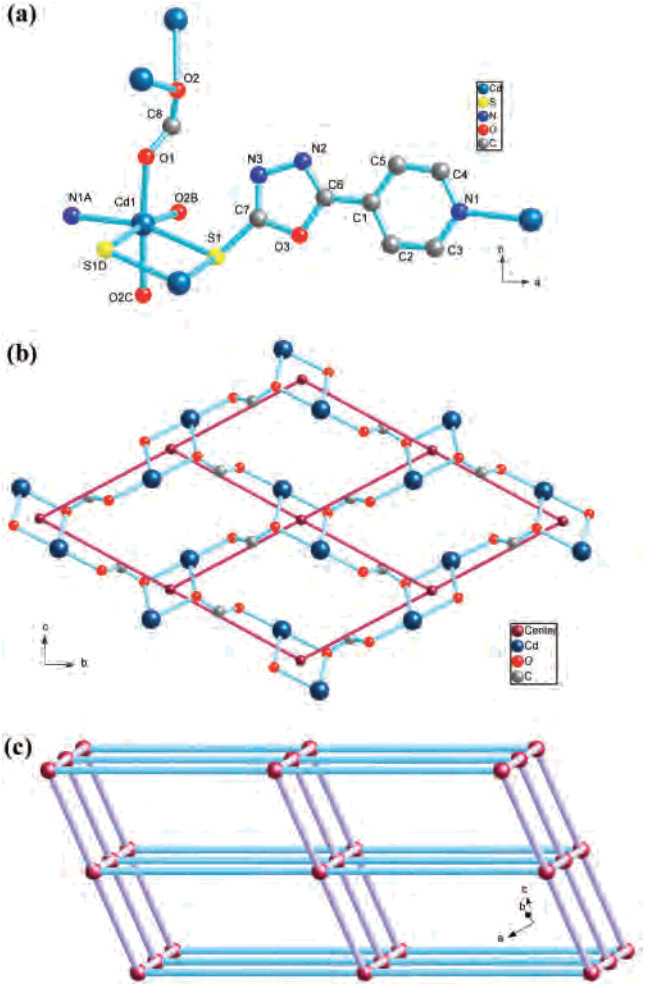

Figure 3. (a) Portion view of **3** with atom labeling of the asymmetric unit and metal-coordination sphere (hydrogen atoms are omitted for clarity). (b) Perspective view of the 2D formate-bridged coordination sheet, together with a schematic diagram of the (4,4) topology, in which the Cd_2O_2 subunits are represented by single nodes. (c) Schematic view of the 6-connected α-Po network topology of **3**.

zole rings. A pair of Cd^{II} atoms is double-bridged by the thiolate groups to form a Cd_2S_2 parallelogram with the Cd···Cd distance of 4.148(2) Å (Figure 3a). As for the formate anions, they connect the Cd^{II} atoms in the μ-O,O$_{anti}$-μ-O,O mode, which facilitates the generation of a 2D sheet. It has a simple (4,4) topology by simplifying each Cd_2O_2 core (Cd···Cd distance = 3.731(2) Å) to a single node (see Figure 3b). These 2D arrays are further linked by pyt as pillars to give a 3D open framework. Each dinuclear node in this network is 6-connected and thus represents a decorated α-Po (4^6) topology (see Figure 3c).[18]

{[Cd(pyt)$_2$]·CHCl$_3$}$_n$ (4). Complex **4** also has a 3D metal−organic framework but with a unique mixed-connected network topology. The asymmetric unit contains one Cd^{II} atom, two pyt anions, and a chloroform solvent. Each octahedral Cd^{II} is bound to six pyt (Figure 4a) via two pyridyl nitrogens, two oxadiazole nitrogens, and two exocyclic sulfurs. Both pyt ligands are in the thioamide form (see Table 3 for bond parameters), and the dihedral angles between the pyridyl and oxadiazole planes are 18.0(1) and 8.1(1)°, respectively. Each pyt ligand takes the μ_3-bridging mode and in turn coordinates to three Cd^{II} centers. From the perspective of network topology, each pyt represents a 3-connected node; they connect the 6-connected Cd^{II} nodes (Figure 4b left), resulting in an unprecedented 3D (3,6)-connected net (Figure 4b right) with Schläfli symbol of $(4^2.6)_2(4^4.6^2.8^7.10^2)$.[18] So far, a variety of uninodal networks have been reported.[1f] However, higher-dimensional nets with mixed connectivity such as (3,6)-, (4,6)-, and (4,8)-connected frameworks are quite rare.[19,20] An analysis of the host voids[17] shows that 33% (708 Å^3) of the unit-cell volume is occupied by the lattice chloroform in the 1D channel along [001] (Figure 4c). Possible weak C−H···S interactions involving pyridyl/chloroform groups and exocyclic sulfur atoms are listed in the Supporting Information, Table S1.

The anionic component hydroxyl or formate is detected in the structure of **1** or **3**, obtained under the solvothermal

(18) (a) Delgado-Friedrichs, O.; O'Keeffe, M. *J. Solid State Chem.* **2005**, *178*, 2499−2504. (b) Wells, A. F. *Three-Dimensional Nets and Polyhedra*; Wiley: New York, 1977.

(19) O'Keeffe, M.; Eddaoudi, M.; Li, H.; Reineke, T.; Yaghi, O. M. *J. Solid State Chem.* **2000**, *152*, 3−20.

(20) (a) Chun, H.; Kim, D.; Dybtsev, D. N.; Kim, K. *Angew. Chem., Int. Ed.* **2004**, *43*, 971−974. (b) Natarajan, R.; Savitha, G.; Dominiak, P.; Wozniak, K.; Moorthy, J. N. *Angew. Chem., Int. Ed.* **2005**, *44*, 2115−2119.

Table 3. Selective Bond Lengths (Å) and Angles (deg) for Complexes **3** and **4**

		3[a]	
Cd1−O1	2.244(2)	Cd1−N1A	2.302(2)
Cd1−O2B	2.311(2)	Cd1−O2C	2.373(2)
Cd1−S1	2.675(1)	Cd1−S1D	2.776(1)
N2−C6	1.290(3)	N3−C7	1.296(3)
S1−C7	1.714(2)		
O1−Cd1−N1A	96.60(7)	O1−Cd1−O2B	103.91(6)
N1A−Cd1−O2B	94.63(8)	O1−Cd1−O2C	177.29(5)
N1A−Cd1−O2C	85.68(6)	O2B−Cd1−O2C	74.39(6)
O1−Cd1−S1	95.24(5)	N1A−Cd1−S1	163.35(5)
O2B−Cd1−S1	93.82(6)	O2C−Cd1−S1	82.83(5)
O1−Cd1−S1D	82.81(5)	N1A-Cd1−S1D	88.98(6)
O2B−Cd1−S1D	171.90(4)	O2C−Cd1−S1D	98.72(5)
S1−Cd1−S1D	80.93(5)	N3−C7−S1	131.5(2)
		4[b]	
Cd1−N1	2.396(2)	Cd1−N3A	2.383(2)
Cd1−N4B	2.394(2)	Cd1−N6C	2.395(2)
Cd1−S1D	2.6561(8)	Cd1−S2	2.7131(7)
C7−S1	1.698(3)	C14−S2	1.698(3)
C7−N3	1.309(4)	N2−C6	1.286(4)
C14−N6	1.310(4)	N5−C13	1.279(4)
N1−Cd1−N3A	97.36(8)	N1−Cd1−N4B	176.04(8)
N1−Cd1−N6C	83.21(8)	N1−Cd1−S1D	87.57(6)
N1−Cd1−S2	92.29(6)	N3A−Cd1−N4B	84.62(8)
N3A−Cd1−N6C	91.30(8)	N3A−Cd1−S1D	87.19(6)
N3A−Cd1−S2	167.15(6)	N4B−Cd1−N6C	100.20(9)
N4B−Cd1−S1D	89.11(6)	N4B−Cd1−S2	86.27(6)
N6C−Cd1−S1D	170.39(6)	N6C−Cd1−S2	81.41(6)
S1D−Cd1−S2	101.73(2)	N3−C7−S1	130.9(2)
N6−C14−S2	131.2(2)		

[a] Symmetry codes: A = $x-1, y, z-1$; B = $x, -y+3/2, z-1/2$; C = $-x, y-1/2, -z+1/2$; D = $-x, -y+1, -z+1$. [b] Symmetry codes: A = $-x, y+1/2, -z+1/2$; B = $-x+1, -y+1, -z$; C = $x, -y+1/2, z+1/2$; D = $-x, -y, -z$.

conditions, which may lead to the generation of compact networks with no or small void volumes accessible.[21] However, under ambient circumstances, the assemblies proceed in different ways to afford two distinct frameworks **2** and **4** with potential porosity. So we deduce that low temperature and slow diffusion may facilitate the capture of organic media molecules by host frameworks with suitable cavities. Besides the synthetic method, the nature of the metal center (Zn^{II} or Cd^{II}) is also evidently responsible for the structural diversification of this new class of metal−organic frameworks. Especially, in the distinct net structures of **2** and **4**, both Zn^{II} and Cd^{II} centers are six-coordinated; however, they behave as the 4- and 6-connected nodes, respectively. This should be attributed to the larger ion radius of Cd^{II} compared with that of Zn^{II}, which may provide enough space to accommodate six concomitant pyt ligands. Anyway, the resulting crystalline materials in this work are well-regulated by either the synthetic routes or metal natures at a time.

Structural Features of the Ligand. From the above descriptions, we can clearly see that despite the rigid skeleton, the versatile pyt building block exhibits changeable coordination modes and a flexible self-modulation nature (either thioamide or thiolate isomer). In this study, the C−S bond lengths for the pyt linker in **1**, **2**, and **4** cover the range of 1.658(2)−1.698(3) Å, whereas the corresponding value in **3** (thiolate) is 1.714(2) Å. Interestingly, the thioamide nitrogen is always coordinated to the Zn^{II} or Cd^{II} center, and the C−N bonds (1.307(3)−1.318(2) Å) are elongated compared with those of the oxadiazole C−N moiety (∼1.29 Å). According to previous results, the oxadiazole nitrogen unfavorably binds to metal ions[22] except for silver(I);[23] only several cases are observed for copper(II) and nickel(II), however, with the aid of the chelating-driven effect.[24] Thus, a bidentate μ-N_{py}, *S*, *S* bridging mode for pyt in **3** (**IV**, see Scheme 2) is easy to understand. Significantly, the coordination fashions of pyt as the thioamide isomer are diversiform, relying on the metal ion as well as the synthetic route. In **1**, a 1D Zn^{II} chain with tridentate pyt (**II**, μ-N_{py},N_{oxa},*S*) is formed, and further expansion is prevented by the monodentate pyt terminals (**I**, η-N_{oxa}). As for **2**, each pyt acts as a rodlike connector (**III**, μ-N_{py},N_{oxa}), affording a layered Zn^{II} polymer; for **4**, all pyt ligands are triconnected nodes via three potential binding sites (**II**), giving a unique 3D (3,6)-connected network. It is predicted that a great variety of coordination modes of pyt will emerge with the increasing number of metal−organic frameworks based on this versatile ligand.

Thermal Stability and Porosity of the New Materials. Thermogravimetric analysis (TGA) experiments were conducted to determine the thermal stabilities of **1**−**4**, which is an important aspect for metal−organic frameworks. For complex **1**, the first weight loss occurs in the range of 160−240 °C (peak: 228 °C). Two consecutive weight losses then start at 310 °C and do not end until heating to 800 °C (peaking positions: 377 and 520 °C). For **2**, the TGA curve shows the weight loss of lattice DMF (calcd: 24.20%; observed: 23.85%) in the temperature range of 50−130 °C (peak: 98 °C). The residual host framework starts to decompose beyond 175 °C along with a series of complicated weight losses (peaks: 292, 322, 380, and 434 °C), which do not end until heating to 800 °C. In the case of **3**, the coordinated framework is stable up to 260 °C, followed by four consecutive steps of weight losses (peaking positions: 287, 337, 472, and 637 °C) of the pyt and formate components until 705 °C. The residue remains 38.31 wt % of the total sample and appears to be CdO (calcd: 38.26%). For the 3D porous complex **4**, a weight loss of 19.59% in 28−86 °C (peak: 56 °C) corresponds to the release of the chloroform guests (calcd: 20.30%). The guest-free microporous framework keeps stable upon further heating until two consecutive weight losses occur in 282−800 °C (peaks: 301 and 319 °C).

The structural analysis and TGA results reveal the potential porous nature of complexes **2** and **4**. To further investigate the porosity, we placed a fresh sample of **2** or **4** in a quartz tube and dried it under a high vacuum at 160 °C for 4 h to exclude the guest solvates, which was evidenced by weight loss of the sample and elemental analysis. The resulting coordination frameworks have no change in conformity to the XRPD patterns of the evacuated solids (Figure 5), which

(21) Choi, E. Y.; Kwon, Y.-U. *Inorg. Chem.* **2005**, *44*, 538−545.

(22) Du, M.; Guo, Y.-M.; Chen, S.-T.; Bu, X.-H.; Batten, S. R.; Ribas, J.; Kitagawa, S. *Inorg. Chem.* **2004**, *43*, 1287−1293 and references therein.

(23) (a) Dong, Y. B.; Cheng, J. Y.; Huang, R. Q.; Smith, M. D.; zur Loye, H. C. *Inorg. Chem.* **2003**, *42*, 5699−5706. (b) Du, M.; Zhao, X.-J.; Guo, J. H.; Batten, S. R. *Chem. Commun.* **2005**, 4836−4838.

(24) (a) Gueddi, A.; Mernari, B.; Giorgi, M.; Pierrot, M. *Acta Crystallogr., Sect. C* **2000**, *56*, e426−e428. (b) Bu, X.-H.; Liu, H.; Du, M.; Zhang, L.; Guo, Y.-M. *Inorg. Chem.* **2002**, *41*, 1855−1861. (c) Catalano, V. J.; Craig, T. J. *Inorg. Chem.* **2003**, *42*, 321−334. (d) Klingele, M. H.; Brooker, S. *Coord. Chem. Rev.* **2003**, *241*, 119−132. (e) Du, M.; Zhao, X. J.; Guo, J. H. *J. Mol. Struct.* **2004**, *702*, 55−59.

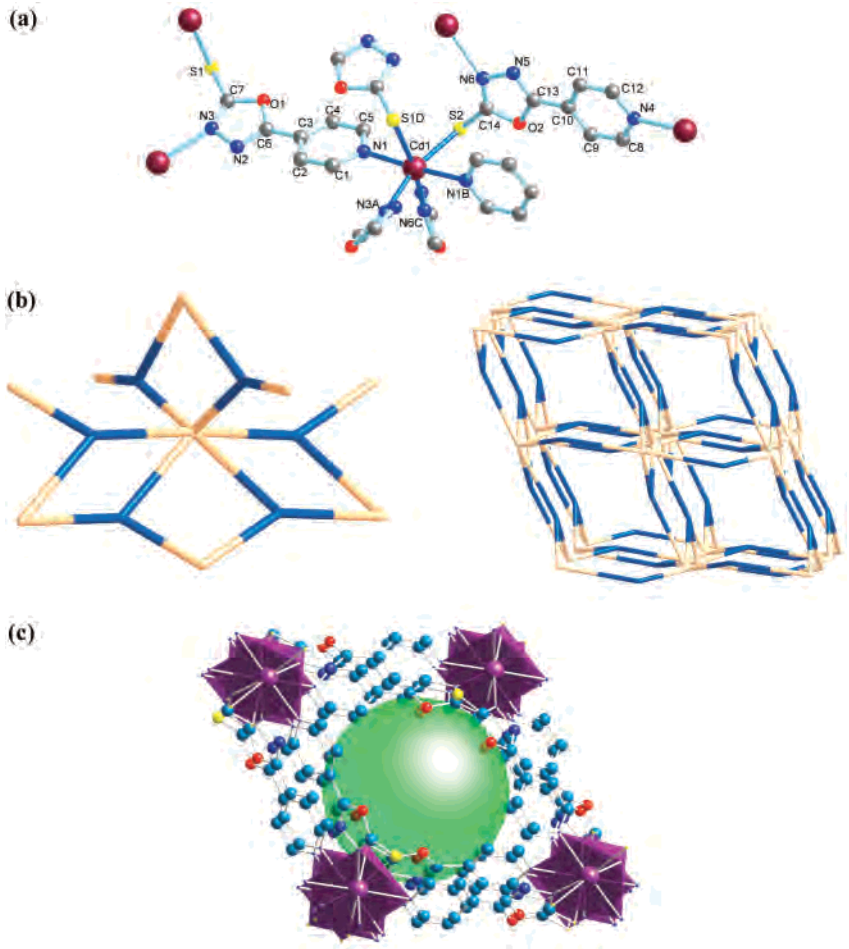

Figure 4. (a) Portion view of **4** with atom labeling of the asymmetric unit and metal-coordination sphere (hydrogen atoms and lattice solvates are omitted for clarity). (b) (left) Schematic presentation of metal and ligand linkages; (right) schematic view of the 3D (3,6)-connected network of $(4^2.6)_2(4^4.6^2.8^7.10^2)$ topology, with blue nodes representing the anionic ligands and orange ones the metal centers. (c) View of the 1D channel along [001] (the green ball represents an included chloroform).

Scheme 2

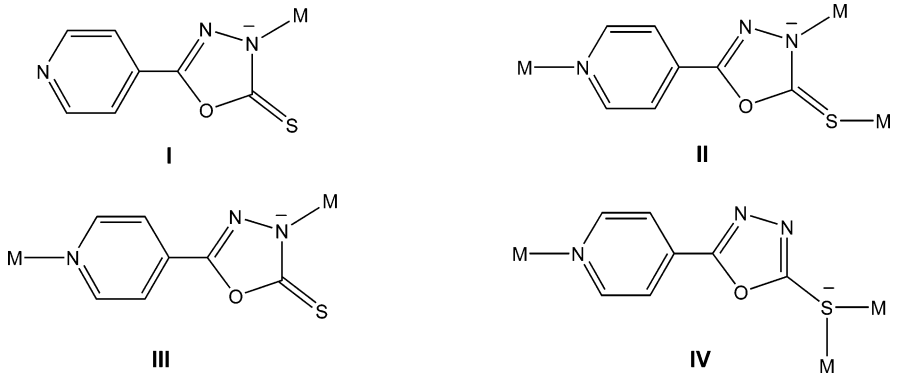

are essentially identical to those of the intact material **2** or **4**. These results clearly demonstrate that the elimination of the solvate guests in **2** and **4** leads to the generation of new microporous materials, which retain the framework integrity of the original crystalline solids. To confirm their permanent porosity, the adsorption properties of the guest-free samples for N_2 with a kinetic diameter of 3.64 Å[25] have been measured at 77 K. As shown in Figure 6, a very small quantity of gas was adsorbed with an approximate value of 22.8 or 8.6 mL per 1.0 g of the desolvated sample of **2** or **4** at 1 atm, although a higher sorption capacity may be possible under higher pressures. Nevertheless, adsorption and desorption curves trace almost the same isotherm, indicating that the framework is retained during this process. This is also suggested from their XRPD patterns. The BET surface area of **2** or **4** is calculated to be only 5.19 or 3.25 m^2/g, evidently being less than a typical value for microporous MOFs. On the other hand, the given microporous volumes

(25) Beck, D. W. *Zeolite Molecular Sieves*; Wiley & Sons: New York, 1974.

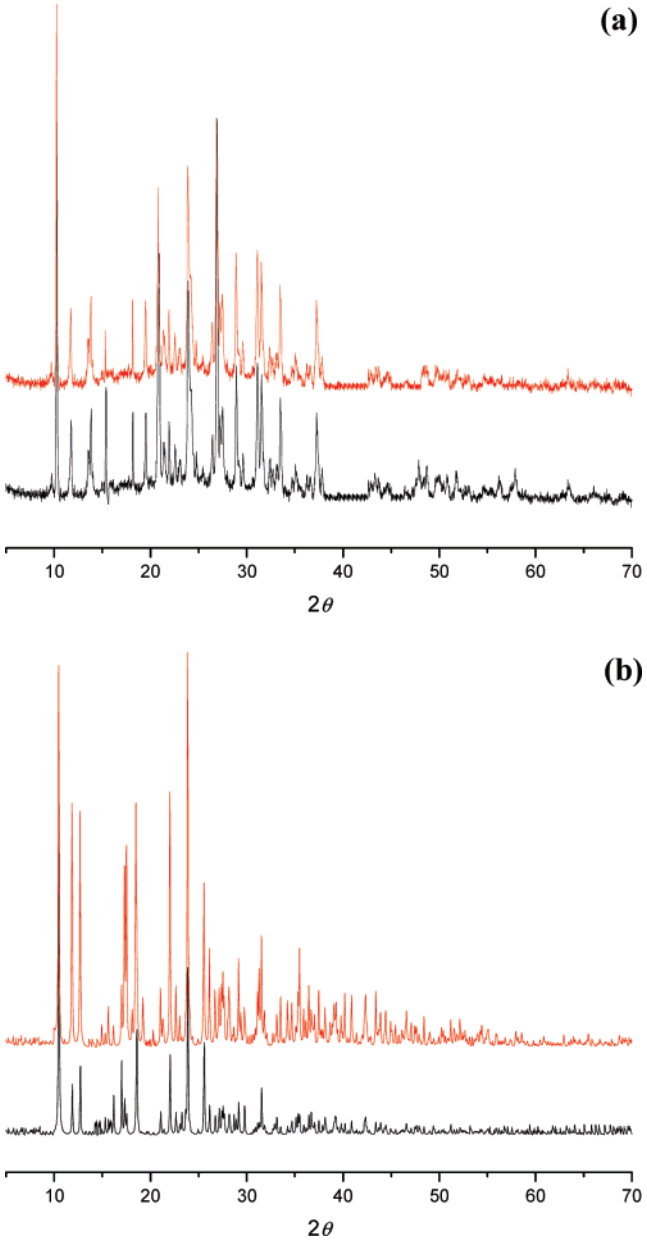

Figure 5. XRPD patterns for (a) **2** and (b) **4**. (black) Recorded at room temperature with a fresh sample; (red) after removal of the guest solvates.

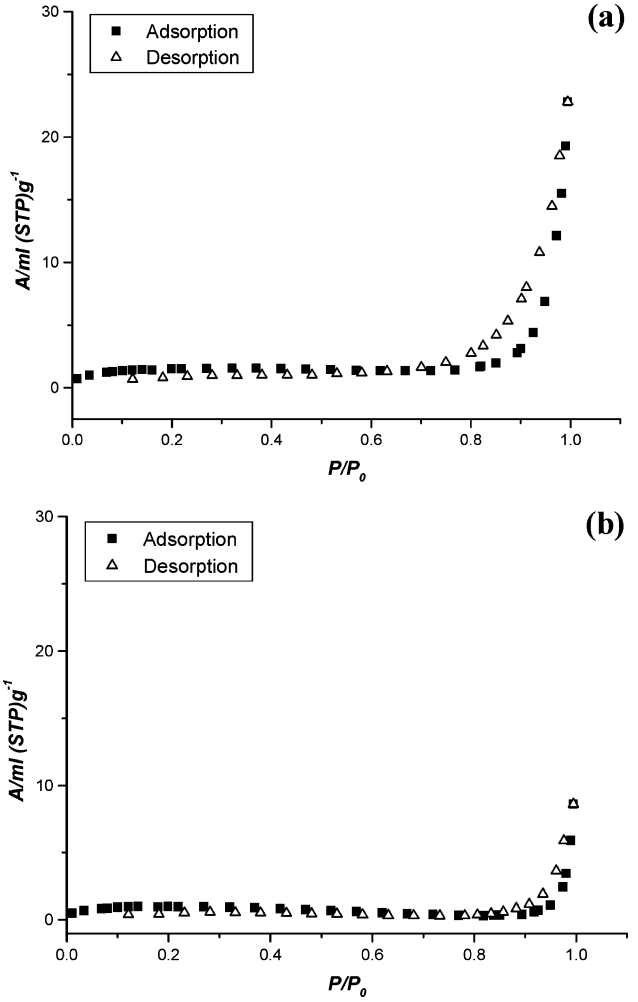

Figure 6. Isotherms for the adsorption and desorption of N_2 at 77 K for (a) **2** and (b) **4**. Herein, A refers to absolute adsorption and STP to standard temperature and pressure.

are only 1.103×10^{-3} cm^3/g for **2** and 1.163×10^{-3} cm^3/g for **4**. These results reveal that only surface adsorption may occur in both cases; that is, the nitrogen molecule could not diffuse into the inner channels of these solids freely despite the fact that they possess stable frameworks and large cavities.

Conclusions and Perspectives

A series of polymeric metal−organic coordination polymers generated from a multidentate oxadiazole-functionalized ligand Hpyt and Zn^{II} or Cd^{II} salts, which interestingly display diverse network structures from 1D zigzag, 2D grid, 3D pillar-layer to 3D (3,6)-connected network, have been prepared and structurally determined. Significantly, this work allows us to see that the polymerization of a metal ion with pyt is tunable through control of the reaction conditions. Although pyt has a rigid backbone, it still shows coordinative versatility with different metal centers because of its multipotential donating sites and changeable isomers, and a systematic research of this interesting ligand with other metal ions is desirable. Of further importance, this work may initiate the coordination chemistry study of a new class of organic ligands with the concurrence of oxadiazole, sulfur, and other heterocyclic functional groups. Further investigation on this perspective is also ongoing, which may provide new opportunities of coordination polymers with novel structures and useful properties.

Acknowledgment. This work was financially supported by the National Natural Science Foundation of China (20401012), the National Fundamental Research Project of China (2005CCA01200), the Key Project of Tianjin Natural Science Foundation (043804111), and the Key Project of Chinese Ministry of Education (No. 205008).

Supporting Information Available: X-ray crystallographic files (CIF) for **1**−**4**, calculated and experimental X-ray powder diffraction (XRPD) patterns for **1**−**4**, an additional figure for **1**, and a table including possible hydrogen-bonding parameters in **2** and **4**. This material is available free of charge via the Internet at http://pubs.acs.org.

IC060129V